Journal of Molecular Catalysis B: Enzymatic 61 (2009) 80–87

Contents lists available at ScienceDirect

Journal of Molecular Catalysis B: Enzymatic

journal homepage: www.elsevier.com/locate/molcatb

Role of 2-oxoglutarate dehydrogenase in brain pathologies involving glutamate neurotoxicity

Anastasia Graf[b], Maria Kabysheva[a], Eugeny Klimuk[a], Lidia Trofimova[b], Tatiana Dunaeva[b], Gregor Zündorf[d], Stefan Kahlert[d], Georg Reiser[d], Tatiana Storozhevykh[c], Vsevolod Pinelis[c], Natalia Sokolova[b], Victoria Bunik[a,*]

[a] Belozersky Institute of Physico-Chemical Biology, Lomonosov Moscow State University, 119992 Moscow, Russian Federation
[b] Physiology Department of Biology Faculty, Lomonosov Moscow State University, 119992 Moscow, Russian Federation
[c] Research Center for Children's Health, Russian Academy of Medical Sciences, 119991 Moscow, Russian Federation
[d] Institut fur Neurobiochemie, Medizinische Fakultat, Otto-von-Guericke-Universitat Magdeburg, 39120 Magdeburg, Germany

ARTICLE INFO

Article history:
Available online 5 March 2009

Keywords:
Glutamate
Hypoxia
2-Oxoglutarate dehydrogenase
Phosphonate analog of 2-oxoglutarate
Sexual differentiation

ABSTRACT

Decreased activity of the mitochondrial thiamin-dependent 2-oxoglutarate dehydrogenase complex (OGDHC) is associated with a number of inborn and acquired neuropathologies. We hypothesized that perturbation in flux through the complex influences brain development and function, in particular, because the OGDHC reaction is linked to the synthesis/degradation of neurotransmitters glutamate and GABA. Developmental impact of this metabolic knot was studied by characterizing the brain OGDHC activity in offspring of rats exposed to acute hypobaric hypoxia at a critical organogenesis period of pregnancy. In this model, we detected the hypoxia-induced changes in the brain OGDHC activity and in certain physiologic and morphometric parameters. The changes were mostly abrogated by application of specific effector of cellular OGDHC, the phosphonate analog of 2-oxoglutarate (succinyl phosphonate), shortly before hypoxia. The glutamate excitotoxicity known to greatly contribute to hypoxic damage was alleviated by succinyl phosphonate in situ. That is, the delayed calcium deregulation, mitochondrial depolarization and reactive oxygen species (ROS) production became less pronounced in cultivated neurons loaded with succinyl phosphonate. In vitro, succinyl phosphonate protected OGDHC from the catalysis-induced inactivation. Thus, the protective effects of the phosphonate upon hypoxic insult in vivo may result from the preservation of mitochondrial function and Ca^{2+} homeostasis due to the phosphonate inhibition of both the OGDHC-dependent ROS production and associated OGDHC inactivation. As a result, we showed for the first time that the hypoxia- and glutamate-induced cerebral damage is linked to the function of OGDHC, introducing the phosphonate analogs of 2-oxoglutarate as promising diagnostic tools to reveal the role of OGDHC in brain function and development.

1. Introduction

A number of inborn and acquired neuropathologies are associated with decreased activity of the mitochondrial 2-oxoglutarate dehydrogenase multienzyme complex (OGDHC) [1–4], where the thiamine-dependent 2-oxoglutarate dehydrogenase (OGDH) is the starting and rate-limiting component. We hypothesized that perturbation in flux through the complex controls brain development and function through the link of the OGDHC reaction to the synthesis/degradation of excitatory (glutamate) and inhibitory (GABA) neurotransmitters. To study the developmental impact of this metabolic knot, we chose the rat model of acute hypobaric hypoxia at a critical organogenesis period of pregnancy. In this model, a number of behavioral and physiological disorders have been observed in the offspring [5–9], with the glutamate neurotoxicity known to greatly contribute to hypoxic-ischemic encephalopathy ([10,11] and references therein). We therefore employed the model to find out if OGDHC of developing brain is perturbed due to hypoxic insult. We also aimed at alleviating the hypoxic damage to offspring by pre-conditioning of pregnant rats to hypoxia with a specific inhibitor of OGDHC, the phosphonate analog of 2-

Abbreviations: BSS, buffered salt solution; $[Ca^{2+}]_c$, cytoplasmic concentration of calcium ions; ECG, electrocardiogram; FCCP, carbonyl cyanide 4-trifluoromethoxyphenylhydrazone; GABA, γ-amino butyric acid; GFAP, glial fibrillary acidic protein; HBSS, Hank's buffered salt solution; NBM, neurobasal medium; OGDH, 2-oxoglutarate dehydrogenase; OGDHC, 2-oxoglutarate dehydrogenase complex; Oli, oligomycin; PESP, phosphono ethyl succinyl phosphonate; PMSF, phenylmethanesulfonyl fluoride; Rh123, rhodamin 123; ROS, reactive oxygen species; SP, succinyl phosphonate; TCA, tricarboxylic acid; TESP, succinyl phosphonate triethyl ester.

* Corresponding author. Tel.: +7 495 939 44 84; fax: +7 495 939 31 81.
E-mail address: bunik@belozersky.msu.ru (V. Bunik).

1381-1177/$ – see front matter © 2009 Elsevier B.V. All rights reserved.
doi:10.1016/j.molcatb.2009.02.016

oxoglutarate, succinyl phosphonate (SP) [12,13]. To decipher the mechanism of SP action in vivo, we studied its effect on the glutamate-induced impairment in situ, controlling the influence of the OGDHC inhibitor on the three known components of the glutamate neurotoxicity: deregulation of Ca^{2+} homeostasis, irreversible mitochondrial depolarization and ROS production. Finally, we also showed in vitro that SP is able to protect OGDHC from the catalysis-induced inactivation which accompanies the ROS production by the complexes [14] and may be stimulated upon metabolic disbalance under pathological conditions [15,16].

2. Experimental

2.1. Materials

The culture media (MEM, NBM), GlutaMax, B27, antibiotics were from "Gibco", USA; the culture medium TNB-100, stabilized glutamine (N-acetyl-L-alanyl-L-glutamine) and protein–lipid-complex were from Biochrom, Germany; rhodamin 123, acetoxymethyl ether of Fura-2FF, hydroethidine, Hoechst 33342, Mitotracker green and secondary Alexa antibodies were from "Molecular Probes", Netherlands; CoA was from "Gerbu", Germany; anti-glial fibrillary acidic protein (GFAP) and anti-NeuN-antibody were from Chemicon (Hampshire, UK), anti-synaptotagmin-antibody from SYSY (Göttingen, Germany). Succinyl phosphonate and its ethyl ethers were synthesized and purified according to published conditions [13]. Other chemicals were from "Sigma", USA.

2.2. Animal experiments and treatments

Wistar rats were bred, housed and treated according to the international guiding principles as adopted by the Animal Physiology Department of Biology Faculty of the Lomonosov Moscow State University. Pregnant rats weighting 250–300 g each were exposed to hypobaric hypoxia at the 9–10 day of pregnancy by placing in a decompression (altitude) chamber of 3.3 L volume, with a vacuum pump "Mez Mohelnice" (Mohelnice, Czech Republic). Acute hypoxia was achieved by decreasing the atmospheric pressure in 1 min to 145 mm Hg, correspondent to 11500 m altitude. Intranasal application of 0.02 mL succinyl phosphonate (0.2 M water solution of the trisodium salt) in the SP-treated groups or physiologic solution in all reference groups was done 45–50 min before hypoxia. All of the viable offspring (not less than five) from rats showing a low resistance to hypoxia ($\leq$5 min before collapsing due to hypoxia) were taken for analysis. ECG was recorded during 3 min using electrodes implanted subcutaneously under narcosis a day prior to the examination. The mean values of the RR intervals (RR, ms), the percentage of the most frequent RR interval, i.e. the mode amplitude (MoA, %), and the statistical significance of the differences in these parameters in groups were estimated using the home-made software. Reproducibility of the data in independent experiments was shown in the two series of hypoxic treatments.

2.3. Tissue samples

After physiological monitoring has been performed during 8 weeks, the offspring were sacrificed by decapitation (the day 60 p.n.), brains were excised quickly and immersed into ice. Cerebellum and cortex were taken for a separate analysis, as these structural regions may be differentially affected by hypoxia [17,18]. The samples were frozen at −70 °C and used individually for the OGDHC assays (6–10 assays per sample). No significant changes in the OGDHC activity were noticed upon one month storage of the samples at −70 °C.

2.4. Cell cultures

Cerebellar granule cells were prepared from postnatal day 7–8 Wistar rat pups using standard procedure described earlier [19]. Neurons represented about 90% of the cells in the culture and were distinguished from glial cells by morphology and fluorescence change associated with calcium increase in response to glutamate.

Hippocampal neurons were studied within the physiologically relevant mixed culture prepared from three postnatal day-1 Wistar rat pups using standard procedures as described [20]. Responses from single cells were assigned to the neurons after characterization of the cells by morphological criteria and unequivocal identification by immunostaining. Hippocampal neurons have varied dendritic and sometimes branching axonal outgrowth emerging from a stellate cell body (soma or perikaryon). Astrocytes have a flat cell body and are hardly recognizable in the transmission picture. After the measurement, the mixed cultures were marked within the region of interest and fixed with 4% paraformaldehyde. The cell types were identified by double immunostaining as described earlier [20]. For astrocytes we used antibodies against GFAP, for neurons against synaptotagmin and the neuron-specific nuclear protein NeuN. Nuclei were counterstained with 10 μg/mL Hoechst 33342 for 10 min. Stained slides were imaged sequentially with setting the fluorescence microscope to excitation/emission at 380 nm/405 nm; 460 nm/510 nm; 520 nm/590 nm for detection of staining for GFAP, synaptotagmin/NeuN, and Hoechst 33342, respectively.

2.5. Measurement of the glutamate-induced changes in cytosolic calcium and mitochondrial potential in cerebellar granule neurons

Cells were loaded with 6 μM acetoxymethyl ester of Fura-2FF for 1 h in the presence of 0.001% Pluronic F127 in buffered salt solution (BSS), pH 7.4, containing, in mM: NaCl 135, KCl 5, glucose 5, $CaCl_2$ 1.8, $MgCl_2$ 1.0, HEPES 20. During the last 20 min of the incubation 3 μM Rh123 was added to the medium. After the loading, cells were washed with BSS omitting indicators and Pluronic. SP was loaded simultaneously with acetoxymethyl ether of Fura-2FF and was present in cellular media throughout the experiment.

A cell-coated glass was placed in a perfusion chamber (0.2 mL) mounted on the stage of an inverted epifluorescent microscope (Axiovert 200 "Zeiss", Germany) equipped with a CCD camera (SnapCool-fx, USA). Fluorescence intensity was monitored every 20 s at room temperature (24–27 °C). The entire soma of individual neurons was used as a region of interest. Kinetics of the fluorescence changes was studied for the representative 40–50 neurons using Metafluor 6.1 software (Universal imaging corp., USA), with the mean traces of the neuronal sample calculated using Prizm 3.0. Fluorescence images of the cells for Ca^{2+} were acquired at 505 nm emission (15 nm bandwidth) during alternate (in 100–200 ms pulses) excitation at 340 and 380 nm. The background fluorescence levels were determined at each wavelength and subtracted prior to calculating the ratio. Absolute values of $[Ca^{2+}]_c$ were determined using the Grynkiewicz equation [21] and the K_d value of 5 μM for Fura-2FF [22]. For calibration, the cytoplasmic Fura-2FF saturation with calcium was achieved upon addition to the cell incubation medium of 5 μM ionomycin with 10 mM $CaCl_2$. Ca^{2+}-free buffer (1 mM EGTA) with 5 μM ionomycin was used to measure the fluorescence of free Fura-2FF in the cells. Rh123 was excited at 488 nm and emission was detected at 535 nm (10 nm bandwidth). Maximal values of the mitochondrial depolarization were determined as the Rh123 fluorescence intensity after addition of 1 μM FCCP. The glutamate-induced changes in the Rh123 fluorescence were expressed as the percentage of the maximal depolarization after the FCCP addition.

2.6. Single-cell imaging of hippocampal neurons

Single-cell imaging of hippocampal neurons was performed with a Zeiss Axioskop microscope (Zeiss, Germany) using a 20× Achroplan water objective equipped with a Polychrom V monochromator and a charge-coupled device camera (TILL-Photonics, Martinsried, Germany). During experiment, cells were bathed in Hanks balanced salt solution (HBSS) containing in mM: KCl, 5.44; KH_2PO_4, 0.44; Na_2HPO_4, 0.34; $MgCl_2$, 0.49; $MgSO_4$, 0.41; NaCl, 132; HEPES, 10; glucose, 5.56; $NaHCO_3$, 4.17; $CaCl_2$, 1.26. The solution was completely exchanged within 0.5 min by a continuous superfusion system. All effectors and dies were applied by addition to the superfusate via a syringe pump to avoid cross contamination of the tubing system with lipophilic agents. Experiments were performed at 36 °C.

2.7. Measurement of mitochondrial potential in hippocampal neurons

The cationic dye Rh123 was used to monitor the mitochondrial potential as described before [20,23].

2.8. Detection of mitochondrial ROS generation in hippocampal neurons

ROS indicator hydroethidine [24,25] was used. Images were taken every 6 s during excitation at 520 nm with a beamsplitter at 580 nm. Emitted light was collected above 590 nm. To limit the intracellular accumulation of oxidized product and to avoid unwanted interferences, we did not preincubate cells with hydroethidine. Cells were initially superfused with 40 mL/h for 3 min with HBSS alone. After 180 s superfusion was changed to HBSS containing 1 μM hydroethidine alone or 1 μM hydroethidine with 0.1 mM glutamate in the presence or absence of 0.2 mM SP or 0.5 mM TESP. Cellular responses were detected in the area outside the nucleus of neurons, where the fluorescence changes are proportional to the ROS generation. The rates of the fluorescence increase were estimated from the linear part of the kinetic curves (500–1400 s).

2.9. Intracellular localization of ROS induced by glutamate in hippocampal neurons

The cells were treated for 15 min at 37 °C with 0.1 mM glutamate and 1 μM hydroethidine, and washed two times with cold HBSS. Afterwards, 0.1 μM mitochondrial marker Mitotracker green and 5 μg/mL nuclear marker Hoechst 33342 were added for 5 min and washed out two times with cold HBSS. To reveal whether the DNA-bound ethidium fluorescent product formed due to the glutamate-induced ROS was in the nuclear or mitochondrial compartment, transmission pictures and single fluorescence pictures stained with 2-hydroxyethidium, Mitotracker and Hoechst were captured sequentially and merged. The excitation/emission wavelengths were, respectively, 520 nm/590 nm, 460 nm/510 nm, 380 nm/405 nm.

2.10. Partial purification of OGDHC from rat brain

Partial purification of OGDHC from rat brain was done according to [26].

2.11. OGDHC solubilization for the homogenate assays

OGDHC was solubilized from the homogenized tissue by sonication followed with a mild detergent extraction. All procedures were done on ice. Cold Buffer 1, including in mM: MOPS (pH 7.0) 50, EGTA 0.2, PMSF 0.5, benzamidinium chloride 1, leupeptin 0.01, dithiothreitol 1, was added to frozen samples at a ratio 1 mL to 400 mg of tissue. Homogenization was done in a small (3 mL) Potter homogenizer with a teflon pestle using the motor-driven rotation during 5 min at a middle power. The homogenate aliquotes (0.3 mL) were placed in 1.5 mL Eppendorf tubes and sonicated in a "Bioruptor" sonicator ("Diagenode", Liege, Belgium) using ice cooling. The six closed Eppendorf tubes in a rotating plate were subject to the three sonication cycles at high power for 30 s with 90 s pause. Sonicated homogenates were diluted 2-fold with Buffer 1. The OGDHC solubilization of the samples was completed by adding one volume of Buffer 2 to the three volumes of the homogenate and incubation for at least 20 min before the assay. Buffer 2 included, in mM: Tris–HCl (pH 7.4) 50, NaCl 150, EDTA 1, PMSF 1, benzamidinium chloride 1, Pefablock 0.2, and sodium deoxycholate 0.25%, NP-40 1%, aprotinin 1 μg/mL, leupeptin 1 μg/mL, pepstatin 1 μg/mL.

2.12. OGDHC and OGDH assays

Reaction rates of OGDHC were determined by the accumulation of the reaction product NADH at 340 nm. Control experiments showed no significant NADH oxidation by the analyzed samples under conditions of the OGDHC assay. Brain homogenates were assayed in the 50 mM MOPS (pH 7.0) including in mM: 2-oxoglutarate 2, thiamine diphosphate 1, $MgCl_2$ 1, coenzyme A 0.1, NAD^+ 2.5, dithiothreitol 1, $CaCl_2$ 1. Purified OGDHC was assayed in 0.1 M potassium phosphate (pH 7.0) containing in mM: 2-oxoglutarate 2, thiamine diphosphate 1, $MgCl_2$ 1, coenzyme A 0.1, NAD^+ 2.5, dithiothreitol 1 mM. 6–12 μL of the homogenate or 1–2 μL of the partially purified sample were added to the total 600 μL of the OGDHC assay medium. The product accumulation curves were followed for 3–5 min, with the linear part of the curve used to calculate the reaction rates as micromole of NADH (molar extinction coefficient 6220 M^{-1} cm^{-1}) generated per minute. OGDH was assayed with an artificial electron acceptor potassium hexacyanoferrate (III) as in [2] by following the absorbance decrease at 420 nm (molar extinction coefficient 1000 M^{-1} cm^{-1}). Kinetics of the product accumulation curves was analyzed as in [27,28]. Optical changes were followed using an Uvikon spectrophotometer (Kontron Instruments, Neufahrn, Germany).

2.13. Statistical analysis

Data are reported as means ± SEM. Statistical analysis was performed by the unpaired two-tailed Student's *t* test using SigmaPlot Ver.10 Systat Software, Inc.

3. Results

3.1. Hypoxic/SP treatments of pregnant rats affect the brain OGDHC activity, cortex and cerebellum masses and ECG in offspring

Fig. 1 shows that acute hypobaric hypoxia of pregnant rats with low resistance to hypoxia causes sex-dependent changes in the OGDHC activity in cortex and cerebellum of the 8 week old offspring. The short-term (≤5 min) hypoxic insult to the pregnant rats induces decreased (males, Fig. 1A) or increased (females, Fig. 1B) activity of OGDHC in these brain regions of offspring. Specific inhibitor of OGDHC in cells and tissues, SP [12,13], was shown to decrease both the flux through OGDHC in cells [29] and the tissue oxygen consumption [30]. Thus, the SP-induced impairment of the aerobic metabolism may mimic certain effects of hypoxia. In good accord with this view were the changes in the female offspring,

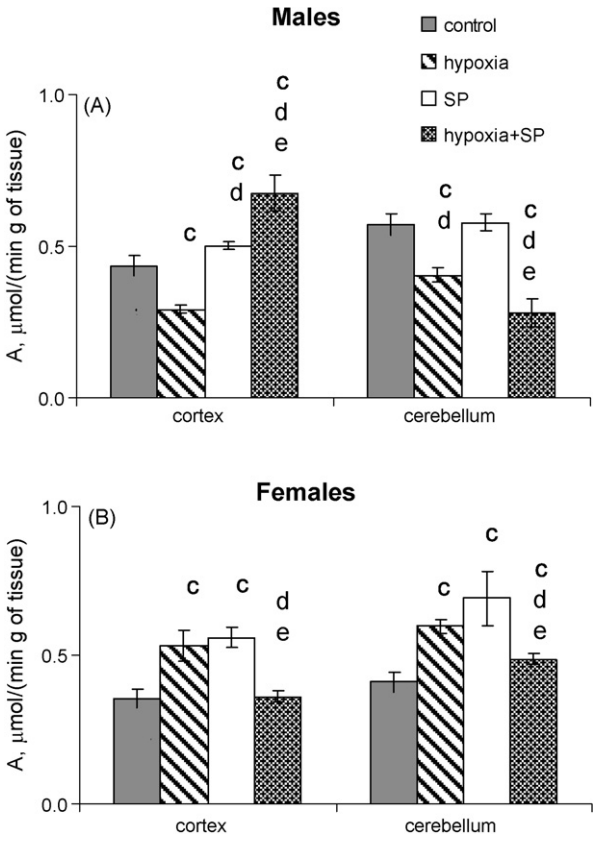

Fig. 1. Influence of the hypoxic, SP and combined treatments of pregnant rats on the OGDHC activity of cortex and cerebellum in the male (A) and female (B) offspring. Activity is expressed as μmol of NADH formed per min g of tissue. Number of assays in groups (n) is from 30 to 50. Statistically significant results with $p < 0.05$ are marked by letters: c—compared to the control group; d—compared to the SP-treated group; e—compared to the hypoxia-affected group.

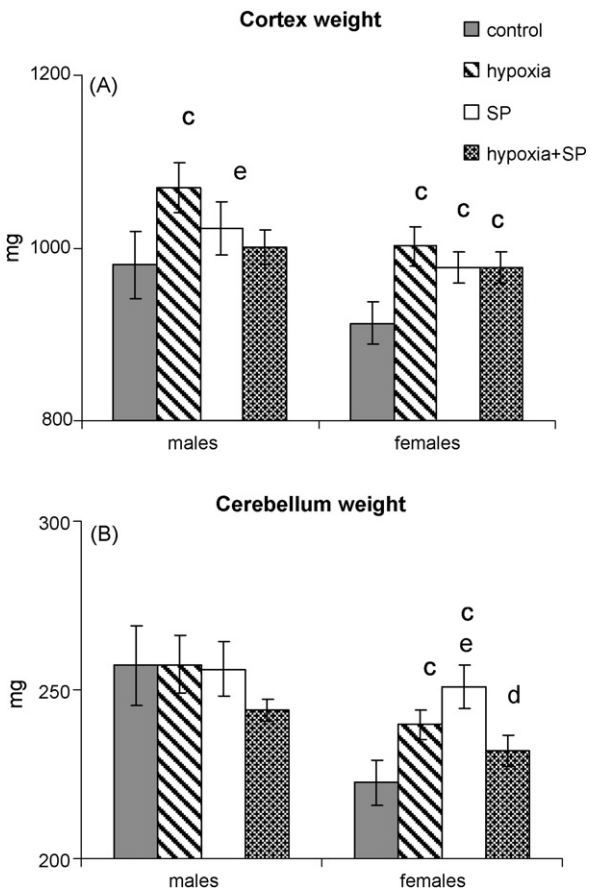

Fig. 2. Influence of the hypoxic, SP and combined treatments of pregnant rats on the masses of cortex (A) and cerebellum (B) in the male and female offspring. Number of brain structures in groups (n) is from 5 to 10. Statistically significant results with $p < 0.05$ are marked by letters as in Fig. 1.

who exhibited a similar increase in their brain OGDHC activity in response to both the hypoxic insult and SP treatment of the pregnant rats (Fig. 1B). In contrast, in the male offspring, where the brain OGDHC was reduced by hypoxia, the activity was resistant to the SP treatment, remaining close to the control values (Fig. 1A). The sex-dependence in the OGDHC reactivity to SP and hypoxia correlated with the originally different control levels of the OGDHC activity in males and females. The lower control activities in female cortex and cerebellum (0.35 ± 0.03 and 0.41 ± 0.02 μmol/(min g of tissue), Fig. 1B) showed approximately 50% increase in response to hypoxia (to 0.53 ± 0.05 and 0.60 ± 0.02 μmol/(min g of tissue), Fig. 1B) or 60–70% increase by SP (to 0.56 ± 0.03 and 0.69 ± 0.09 μmol/(min g of tissue), Fig. 1B). This up-regulation of the activity due to hypoxia or SP was not observed in males (Fig. 1A), probably due to the fact that in males already the control OGDHC levels (0.44 ± 0.03 and 0.57 ± 0.04 μmol/(min g of tissue), Fig. 1A) were 30–40% higher than in females.

Morphometric analysis of the studied brain structures showed that hypoxia increased the mass of cortex in both males and females and of cerebellum in females (Fig. 2). Thus, the hypoxia effects on the offspring brain were evident on both biochemical (perturbation in the OGDHC activity) and morphometric (masses of cortex and/or cerebellum) levels. Similar to hypoxia, SP increased the masses of both cortex and cerebellum in females. In males, a weaker response of the masses to hypoxia (only in cortex, and with a low statistical significance, i.e. at $p < 0.17$) was accompanied by no significant change of the masses by SP treatment (Fig. 2). This correlated with no changes by SP in the brain OGDHC activity of males (Fig. 1). Thus, according to both the morphometric parameters and OGDHC assays, the female brain was more responsive to SP than the male brain. Unlike the sex-dependent changes in the OGDHC activity and mass in brain, the functional activity of the cardiovascular system was affected similarly in both male and female offspring. That is, SP or hypoxia increased RR interval and decreased mode amplitude of ECG in both sexes (Fig. 3).

3.2. SP interference with hypoxic effects on offspring

Combined action of SP and hypoxia showed non-additive antagonistic relationship between the two insults in most cases. That is, except for the OGDHC activity in the male cerebellum, treatment of pregnant rats with SP before hypoxia opposed the OGDHC changes induced by hypoxia (Fig. 1). In the female offspring, the SP pre-conditioning resulted in the preservation of the OGDHC activity at its normal levels (Fig. 1B). In cortex of the male offspring, the OGDHC activity decrease after hypoxia was also opposed by the SP pre-conditioning, but the OGDHC activity increased beyond the control levels (Fig. 1A). Non-additive antagonistic action of SP and hypoxia was also observed in the morphometric and physiologic parameters (Figs. 2 and 3). The combined action of SP and hypoxia tended to normalize these parameters, similar to their action on the brain OGDHC activity (Fig. 1). In particular, the SP pre-conditioning returned to normal the masses of the cortex in males (Fig. 2A), of the cerebellum in females (Fig. 2B), the RR interval in males (Fig. 3A) and mode amplitude in females (Fig. 3B).

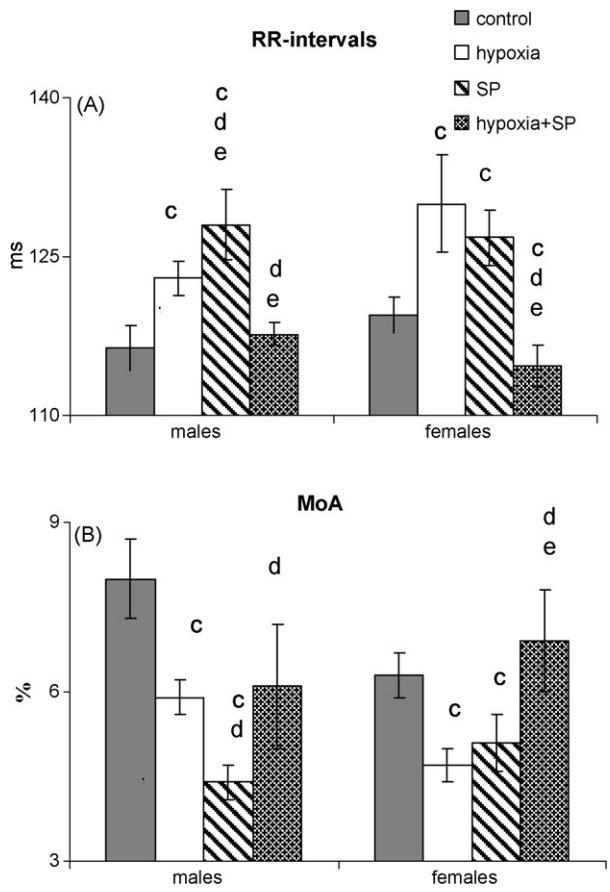

Fig. 3. Influence of the hypoxic, SP and combined treatments of pregnant rats on the ECG parameters RR interval (A) and mode amplitude (B) of the male and female offspring. Number of animals in groups (n) is from 5 to 27. Statistically significant results with $p < 0.05$ are marked by letters as in Fig. 1.

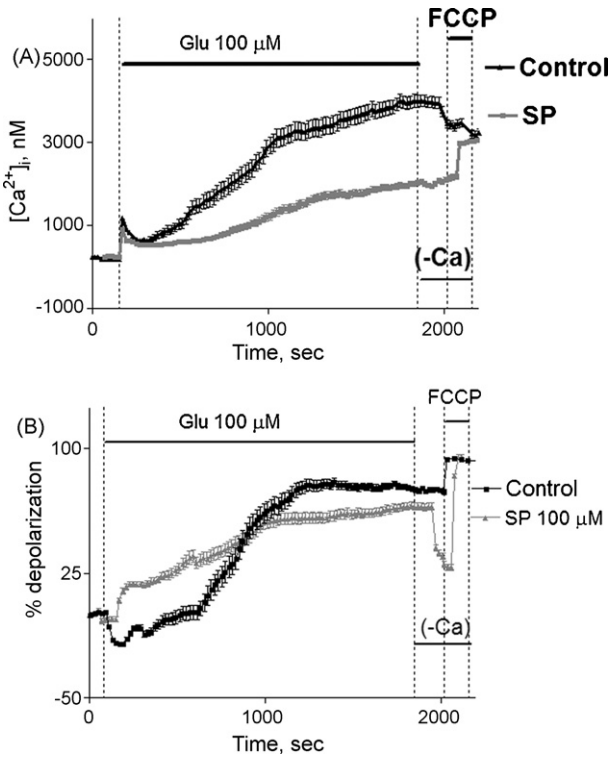

Fig. 5. Averaged glutamate-induced changes in cytoplasmic calcium $[Ca^{2+}]_c$ (A) and mitochondrial potential (B) of the samples of control neurons (black line) and neurons preincubated for 1 h with 0.1 mM SP (grey line). The curves represent mean traces of 40 control or SP-loaded neurons. Experimental condition details are as in Fig. 4.

3.3. SP alleviates the glutamate excitotoxicity in situ

Hypoxic insult is known to involve the glutamate excitotoxicity ([10,11] and references therein). It was therefore of special interest whether the alleviation of the hypoxic effects observed upon the SP pre-conditioning of pregnant rats (Figs. 1–3) would correlate with the SP action in cellular model of glutamate excitotoxicity. Fig. 4 shows typical changes in cytoplasmic calcium (black line) and mitochondrial potential (grey line) of single neurons in such a model. The excitotoxic action is developed upon prolonged incubation of cerebellar granule neurons with 0.1 mM glutamate in the Mg^{2+}-free, glycine-supplemented medium. As shown before [31,32], under these conditions neurons respond to glutamate by a rapid transient increase in $[Ca^{2+}]_c$, which is followed by the so-called delayed calcium deregulation. The latter manifests in massive irreversible increase in $[Ca^{2+}]_c$ to a high plateau level, which is accompanied by a strong mitochondrial depolarization (Fig. 4A). The amplitude of the first transient calcium peak, corresponding to the calcium influx through the NMDA receptors [31], was not affected by SP. However, the second phase, i.e. the delayed calcium deregulation, was characterized by several differences between the control and preincubated with SP neurons. The features were obvious upon comparison of both the single-cell traces (Fig. 4) and trend responses of the samples of 40–50 neurons (Fig. 5). Firstly, the control neurons exhibit significantly higher plateau level of $[Ca^{2+}]_c$ (~4000 nM) than the neurons preincubated with SP (~2000 nM) (Figs. 4 and 5A). Secondly, the massive increase in $[Ca^{2+}]_c$ is delayed in the SP-loaded neurons. Thirdly, upon removal of Ca^{2+} from the

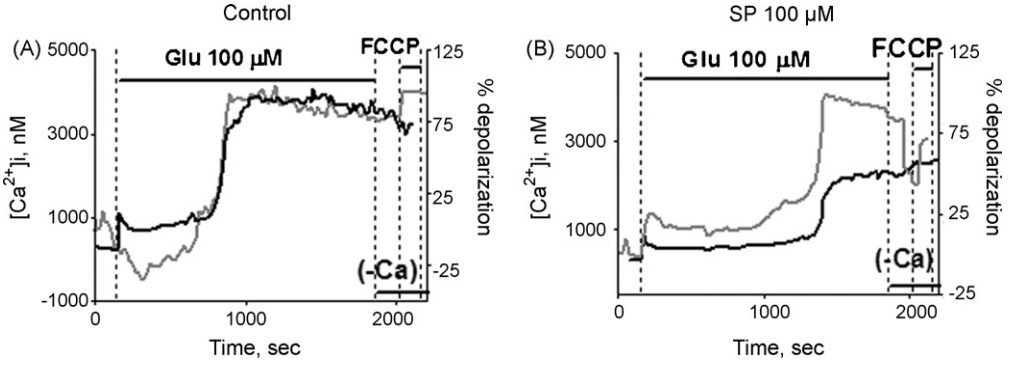

Fig. 4. Cytoplasmic calcium $[Ca^{2+}]_c$ (black line) and mitochondrial potential (grey line) of single cerebellar granule neurons exposed to the prolonged action of excitotoxic concentration of glutamate (0.1 mM) after 1 h preincubation of the cells without (A) or with (B) 0.1 mM SP. Experimental condition details are given in Section 2.5.

medium, the mitochondrial depolarization cannot be reversed in the control neurons, but is reversible in the neurons loaded with SP (Figs. 4 and 5B). As a result, the subsequent addition of an uncoupler (FCCP) causes a significant increase in the Rh123 fluorescence of such neurons which is not observed in the control cells (Figs. 4 and 5B). Thus, the SP-loaded neurons exhibit more resistance against the glutamate excitotoxicity, which manifests in the lower amplitude and delayed onset of the massive increase in $[Ca^{2+}]_c$, and in the reversibility of the accompanying mitochondrial depolarization of neurons.

3.4. SP inhibits the neuronal ROS production induced by glutamate

Another deleterious effect of the prolonged glutamate action on neurons, supposed to contribute to the glutamate neurotoxic effects, is an increase in neuronal ROS production [33,34]. OGDHC is known to generate ROS as by-products of 2-oxoglutarate oxidation at a rate comparable to the established ROS producers [14–16]. Three features of the OGDHC-dependent ROS production may be taken into account to distinguish the OGDHC-specific contribution to neuronal ROS in response to glutamate. Firstly, the primary species produced by OGDHC is $O_2^{\bullet -}$ [14]. Secondly, in situ, this superoxide anion radical should co-localize with OGDHC, i.e. be revealed inside mitochondria, as $O_2^{\bullet -}$ does not penetrate membranes. Thirdly, SP as an OGDHC inhibitor competitive to 2-oxoglutarate should inhibit the 2-oxoglutarate-dependent ROS production by OGDHC. The neuronal formation of ROS was studied under conditions closely resembling physiological ones, i.e. in the mixed culture of hippocampal neurons. To detect their ROS production, we incubated this culture with the cell permeant ROS indicator hydroethidine. When glutamate was added to such neurons, their fluorescence increased significantly more compared to that with hydroethidine alone. The appearance of the fluorescent product pointed to the neuronal generation of the superoxide anion radical, as only this species specifically oxidizes hydroethidine [25]. Because the quantum efficiency of the hydroethidine oxidation product increases 20-fold when it is bound to DNA [24,25,35], the intense fluorescence of the product could be localized to either mitochondria or nucleus. Our study of the co-localization of hydroxyethidium fluorescence with either mitochondrial marker Mitotracker green or nuclear marker Hoechst 33342 (see Section 2.9) showed that the glutamate-induced DNA-2-hydroxyethidium fluorescence was co-localized with Mitotracker, whereas no overlap was detectable with Hoechst 33342. Thus, in accord with a previous study [24], the increase of the fluorescence signal upon incubation of neurons with glutamate in our experimental system results mainly from $O_2^{\bullet -}$ generated in mitochondria. Table 1 shows that production of this intramitochondrial $O_2^{\bullet -}$ is significantly inhibited by SP and its uncharged derivative TESP. The latter was used in anticipation of its better membrane permeability due to the lack of the three negative charges inherent in SP. Although non-inhibiting per se, TESP may be transformed to the OGDHC inhibitors, such as SP and its monoethylated derivatives, by intracellular esterases [13]. Table 1 shows that under chosen conditions the glutamate-induced ROS production was inhibited by about 20% with 0.2 mM SP and 40% with 0.5 mM TESP. Thus, glutamate induces production of superoxide anion radical in neuronal mitochondria, which is inhibited by specific inhibitors of cellular OGDHC. These data point to significant contribution of neuronal OGDHC to the glutamate-induced ROS production. The OGDHC inhibition by the phosphonates under experimental conditions was independently confirmed by a drop in mitochondrial potential of cultivated neurons in the presence of 0.2 mM SP or 0.5 mM TESP. The potential (arbitrary fluorescence units, determined as described in Section 2.7) decreased from 38.8 ± 2.3 in the presence of glutamate alone (control) to 22.0 ± 1.7 or 9.4 ± 2.4 in the presence of glutamate with SP or TESP, respectively.

Table 1
Influence of SP and its triethylated derivative TESP on the rate of neuronal ROS production in the presence of glutamate. The rate was measured as an increase in fluorescence, ΔF/min, of the hydroethidine-loaded hippocampal neurons (see Section 2.8).

Conditions	Rate of ROS production (ΔF/min)
Glutamate 0.1 mM	0.23 ± 0.01
Glutamate 0.1 mM + SP 0.2 mM	0.19 ± 0.01
Glutamate 0.1 mM + TESP 0.5 mM	0.13 ± 0.02

Table 2
Influence of SP on the apparent rate constant of the irreversible inactivation of OGDH in the course of catalysis (k_2, min^{-1}). The OGDH activity was determined in the ferricyanide assay at 1 mM 2-oxoglutarate, and kinetic treatment of the product accumulation curves was performed as described in Section 2.12.

SP (μM)	k_2 (min^{-1})
0	0.20 ± 0.03
0.5	0.08 ± 0.02
5	0.001 ± 0.001

3.5. SP protection from the OGDH inactivation in vitro

It was shown earlier that the OGDHC-dependent ROS generation in the course of catalysis is accompanied by inactivation of the first component of the complex, OGDH [14,16]. On the other hand, decreased activity of OGDHC is associated with neurodegeneration and is supposed to be due to the enzyme inactivation which is promoted under metabolic disbalance [1,15]. Therefore the ability of SP to protect OGDH from the inactivation during catalysis was tested in vitro. Table 2 shows that SP exhibits the concentration-dependent protective effect indeed, with a full protection observed already at a very low SP concentration (0.005 mM).

4. Discussion

In this work, we showed that brain OGDHC in offspring is responsive to hypoxia experienced by pregnant rats at a period critical for the fetal organogenesis (Fig. 1). Our finding thus indicates that the oxidative decarboxylation of 2-oxoglutarate catalyzed by OGDHC is among the metabolic reactions affected in offspring whose development is disturbed due to maternal hypoxia. The changes in activity of this key mitochondrial enzyme complex catalyzing an irreversible degradation of a branch point metabolite and glutamate precursor 2-oxoglutarate points to a persistent perturbation in the brain metabolism of offspring due to hypoxia during pregnancy. Associated morphometric and physiological changes (Figs. 2 and 3) are in accord with known facts that the development of neural system is disturbed upon mutations in OGDHC [3,4] and that the reduced OGDHC activity is associated with neurodegeneration [1]. All these findings point to a critical position of the OGDHC-catalyzed process for the development and function of neural system. The model developed in this work enables further studies to reveal the impact of the brain OGDHC function and regulation on physiology.

Apart from producing energy within the mitochondrial TCA cycle, the OGDHC-catalyzed reaction represents an important branch point, where metabolism of carbohydrates and amino acids intersect through a common intermediate 2-oxoglutarate. Controlling the availability of the 2-oxoglutarate carbon skeleton for the nitrogen assimilation, the sex-dependent expression of the OGDHC activity found in this work (Fig. 1, control males vs. females) obviously contributes to formation of the sex-dependent metabolism in brain. The difference in the brain OGDHC activity should determine,

in particular, the levels of the amino acid-related neuromediators essential for sexual differentiation and behavior, such as serotonine, noradrenaline and dopamine [36]. Obviously, such metabolic differences could be more important in brain than in cardiovascular system. In this regard it is worth noting that the responses of cardiovascular system to hypoxia and/or SP were sex-independent (Fig. 3), in contrast to the responses of the brain morphometric parameters (Fig. 2).

The observed similarity in the effects of hypoxia and the OGDHC inhibitor SP is in good accord with an impairment of glutamate metabolism known to occur in both cases. The OGDHC substrate, 2-oxoglutarate is the direct precursor of glutamate upon de novo synthesis of glutamate from glucose. Accordingly, in a wide range of systems from bacteria to mammals, the glutamate level depends on the OGDHC activity. As the glutamate precursor, 2-oxoglutarate is also linked to the GABA synthesis. In particular, the in situ inhibition of OGDHC by SP resulted in increases in the tissue levels of glutamate and GABA [30], whereas in the animal model of the OGDHC inhibition by a coenzyme analog an increase in extracellular glutamate was observed [37]. Interestingly, when the SP-induced changes in the neuronal pools of glutamate and GABA were determined after washing out the extracellular medium, no change or a slight decrease were observed [29], suggesting an increased excretion of glutamate and GABA upon their intracellular accumulation due to the OGDHC inhibition. Hypoxia also affects the levels of glutamate and GABA [38–40]. Common to hypoxia and the OGDHC inhibition, the perturbation in the tissue glutamate levels is obviously due to impaired glutamate oxidation in the TCA cycle, which occurs when either the flux through OGDHC or oxygen are limited. The resulting glutamate increase may underlie the observed similarity in responses of offspring to application of the OGDHC inhibitor SP or hypoxia in pregnant rats (Figs. 1–3), although due to complexity of the in vivo system this is not obligatory. For instance, in some cases the different responses to SP and hypoxia correlate with the sex-dependent differences in the expression and regulation of OGDHC (Fig. 1). Thus, on one hand, hypoxia affects both the glutamate level [38–40] and brain OGDHC activity (Fig. 1). On the other hand, the OGDHC inhibition affects the tissue glutamate level [30,37] and has developmental impact similar to and/or interfering with hypoxia (Figs. 1–3). It is worth noting in this regard that glutamate is known to regulate proliferation, migration and survival of neuronal progenitors and immature neurons during development [41,42]. This may underlie the observed correlation between perturbations in the OGDHC reaction (Fig. 1) and masses of the brain structures (Fig. 2).

It is of potential therapeutic interest that the combined action of SP and hypoxia led to non-additive and antagonistic effects, with a trend to normalize the offspring parameters affected by hypoxia (Figs. 1–3). Because the glutamate neurotoxicity is a known contributor of hypoxic insult [18,43], and the measured consequences of the insult became less evident upon the SP pre-conditioning (Figs. 1–3), we checked the SP influence on the main components of the glutamate neurotoxicity in situ. As shown in Figs. 4 and 5, preincubation of neurons with SP alleviated the glutamate-induced Ca^{2+} deregulation, preserving mitochondria from irreversible depolarization. Besides, inhibition of neuronal OGDHC by phosphonates reduced the production of the glutamate-induced superoxide anion radical in neuronal mitochondria (Table 1). These data point to a significant contribution of the OGDHC-generated superoxide anion radical to the glutamate-induced ROS production in neurons, in good accord with our earlier in vitro data that OGDHC produces ROS at the expense of 2-oxoglutarate at a rate comparable to the known ROS producers [14]. Because the Ca^{2+} deregulation, irreversible depolarization of mitochondria and elevated production of ROS are known components of the glutamate neurotoxic action, the alleviation of these effects by the OGDHC inhibitor in situ (Figs. 4 and 5 and Table 1) is in good accord with the protection exhibited by SP upon hypoxic insult in vivo (Figs. 1–3). Besides, several independent laboratories showed that inactivation of OGDHC is associated with neurodegeneration [1]. The self-inactivation of OGDH in the course of catalysis [14,27] may be one of the reasons decreasing the overall OGDHC activity under pathological conditions [15,16]. The self-inactivation is particularly stimulated when OGDHC generates ROS at the expense of 2-oxoglutarate [14–16]. Table 2 shows that very low concentrations of SP are able to fully protect OGDH from self-inactivation in vitro. Thus, SP interaction with OGDH may cause at least two immediate effects of the neuroprotective value. First of all, competing with 2-oxoglutarate at the active site of OGDH, SP decreases the 2-oxoglutarate-dependent ROS production, inhibiting elevation of neuronal ROS in the presence of glutamate (Table 1). At the same time, SP protects OGDH from the inactivation (Table 2) which is observed upon the OGDHC-dependent ROS production [14] and may be stimulated in neurodegenerative diseases [1,15]. Thus, SP is able to directly reduce one of the main components of the glutamate neurotoxicity, elevation in the neuronal ROS production, at the same time preserving the OGDHC activity under pathological conditions. The ensuing preservation of the mitochondrial function and calcium homeostasis provides for a mechanism of the neuroprotective action of SP which we observed both in situ (Figs. 4 and 5) and in vivo (Figs. 1–3).

5. Conclusions

Our data indicate a critical significance of OGDHC for the developmental impact of maternal hypoxia, suggesting that regulation of OGDHC may be employed to alleviate hypoxic damage and/or achieve metabolic adaptations to hypoxia. Synthetic analogs of 2-oxoglutarate offer new opportunities to affect this critical metabolic knot in vivo, exposing the potential of specific inhibition of the 2-oxo acid dehydrogenases by the phosphonate analogs of their substrates, known since the introduction of the phosphonate analog of pyruvate to mechanistic studies of thiamine-dependent dehydrogenases [44].

Acknowledgements

We are grateful to Prof. N.K. Lukashev and Dr. A.V. Kazantsev from the Chemistry Department of Moscow Lomonosov State University for synthesis and purification of the phosphonate analogs of 2-oxoglutarate. The work was supported by grants from Russian Foundation of Basic Research (grant 06-08-01441) and Alexander von Humboldt Foundation (DEU/1108773).

References

[1] G.E. Gibson, J.P. Blass, M.F. Beal, V. Bunik, Mol. Neurobiol. 31 (2005) 43–63.
[2] Bunik, G. Raddatz, R.J. Wanders, G. Reiser, FEBS Lett. 580 (2006) 3551–3557.
[3] R.J. Dunckelmann, F. Ebinger, A. Schulze, R.J.A. Wanders, D. Rating, E. Maytepek, Neuropediatrics 31 (2000) 35–38.
[4] A. Amsterdam, R.M. Nissen, Z. Sun, E.C. Swindell, S. Farrington, N. Hopkins, Proc. Natl. Acad. Sci. U.S.A. 101 (2004) 12792–12797.
[5] V.F. Puchkov, Morfologiia 105 (1993) 147–158 (Russian).
[6] C. Nyakas, B. Buwalda, P.G. Luiten, Prog. Neurobiol. 49 (1996) 1–51.
[7] J. Mamet, J. Peyronnet, D. Perrin, Pediatr. Res. 51 (2002) 207–217.
[8] M.V. Johnston, M.E. Blue, S. Naidu, J. Child Neurol. 20 (2005) 759–763.
[9] M. Derrick, A. Drobyshevsky, X. Ji, S. Tan, Stroke 38 (2007) 731–735.
[10] G. Papazisis, C. Pourzitaki, C. Sardeli, A. Lallas, E. Amaniti, D. Kouvelas, Pharmacol. Res. 57 (2008) 73–78.
[11] J. Xie, G. Lu, Y. Hou, Biol. Signals Recept. 8 (1999) 267–274.
[12] V.I. Bunik, A.I. Biryukov, Yu.N. Zhukov, FEBS Lett. 303 (1992) 197–201.
[13] V.I. Bunik, T.T. Denton, H. Xu, C.M. Thompson, A.J.L. Cooper, G.E. Gibson, Biochemistry 44 (2005) 10552–10561.
[14] V. Bunik, C. Sievers, Eur. J. Biochem. 269 (2002) 5004–5015.
[15] V.I. Bunik, J.V. Schloss, J.T. Pinto, G.E. Gibson, A.J. Cooper, Neurochem. Res. 32 (2007) 871–891.
[16] V. Bunik, Eur. J. Biochem. 270 (2003) 1036–1042.

[17] S.K. Hota, K. Barhwal, S.B. Singh, G. Ilavazhagan, Neurochem. Int. 51 (2007) 384–390.
[18] C. Kaur, V. Sivakumar, G. Singh, J. Singh, E.A. Ling, Neuroscience 135 (2005) 1217–1229.
[19] B.I. Khodorov, T.P. Storozhevykh, A.M. Surin, A.I. Iuriavichus, E.G. Sorokina, A.V. Borodin, N.P. Vinskaia, L.G. Khaspekov, V.G. Pinelis, Ross. Fiziol. Zh. Im. I M Sechenova 87 (2001) 459–467.
[20] S. Kahlert, G. Zündorf, G. Reiser, J Neurosci. Res. 79 (2005) 262–271.
[21] G. Grynkiewicz, M. Poenie, R.Y. Tsien, J. Biol. Chem. 260 (1985) 3440–3450.
[22] V.A. Golovina, M.P. Blaustein, Science 275 (1997) 1643–1648.
[23] S. Kahlert, G. Zündorf, G. Reiser, J Neurosci. Methods 171 (2008) 87–92.
[24] V.P. Bindokas, J. Jordan, C.C. Lee, R.J. Miller, J. Neurosci. 16 (1996) 1324–1336.
[25] L. Benov, L. Sztejnberg, I. Fridovich, Free Radic. Biol. Med. 25 (1998) 826–831.
[26] V. Bunik, T. Kaehne, D. Degtyarev, T. Shcherbakova, G. Reiser, FEBS J. 275 (2008) 4990–5006.
[27] V.I. Bunik, O.G. Pavlova, Biochemistry (Moscow) 62 (1997) 973–982.
[28] V.I. Bunik, O.G. Romash, V.S. Gomazkova, FEBS Lett. 278 (1991) 147–150.
[29] S.S. Santos, G.E. Gibson, A.J. Cooper, T.T. Denton, C.M. Thompson, V.I. Bunik, P.M. Alves, U. Sonnewald, J. Neurosci. Res. 83 (2006) 450–458.
[30] W.L. Araujo, A. Nunes-Nesi, S. Trenkamp, V.I. Bunik, A.R. Fernie, Plant physiology, Published online on October 8, 2008, as DOI:10.1104/pp.108.126219.
[31] B.I. Khodorov, Prog. Biophys. Mol. Biol. 86 (2004) 279–351.
[32] D.G. Nicholls, S.L. Budd, Physiol. Rev. 80 (2000) 315–360.
[33] C. Chinopoulos, V. Adam-Vizi, FEBS J. 273 (2006) 433–450.
[34] J.T. Coyle, P. Puttfarcken, Science 262 (1993) 689–695.
[35] H. Zhao, J. Joseph, H.M. Fales, E.A. Sokoloski, R.L. Levine, J. Vasquez-Vivar, B. Kalyanaraman, Proc. Natl. Acad. Sci. U.S.A. 102 (2005) 5727–5732.
[36] A.A. Tkachenko, Abnormal Sexual Behavior, Press center of law, St.-Petersburg, 2003.
[37] A.S. Hazell, R.F. Butterworth, A.M. Hakim, J. Neurochem. 61 (1993) 1155–1158.
[38] L.L. Jantzie, P.Y. Cheung, L. Obaid, M. Emara, S.T. Johnson, D.L. Bigam, K.G. Todd, Resuscitation 77 (2008) 111–120.
[39] Y. Miyashita, A.G. Good, Plant Cell. Physiol. 49 (2008) 92–102.
[40] D.A. Hehre, C.J. Devia, E. Bancalari, C. Suguihara, Pediatr. Res. 63 (2008) 46–50.
[41] H. Komuro, P. Rakic, Science (1993) 95–97.
[42] L. Guerrini, F. Blasi, D. Denis-Donini, Proc. Natl. Acad. Sci. U.S.A. 92 (1995) 9077–9081.
[43] C. Ikonomidou, M.T. Price, J.L. Mosinger, G. Frierdich, J. Labruyere, K.S. Salles, J.W. Olney, J. Neurosci. 9 (1989) 1693–1700.
[44] R. Kluger, D.C. Pike, J. Am. Chem. Soc. 99 (1977) 4504–4506.